Journal of
Ceramic Science
and Technology

J. Ceram. Sci. Tech., **01** [01] 7-14 (2010)
DOI: 10.4416/JCST2010-00003
available online at: http://www.ceramic-science.com

Water Structure Changes within High Solids Loading Calcium Carbonate Slurries

Joshua J. Taylor, Yi-Chung Wang and Wolfgang M. Sigmund*

Department of Materials Science and Engineering, University of Florida, Gainesville, FL 32611
received March 9, 2010; received in revised form May 24, 2010; accepted May 25, 2010

Abstract

Slurries with up to 75 ms% calcite were investigated with attenuated total reflectance – Fourier transform infrared spectroscopy (ATR-FTIR). It was found that infrared absorption bands for water and deuterated water in slurries strongly depend on the solids loading. As the solids loading increases there is a decrease in structured water. Aging of the slurry reverses the trend and increases the amount of structured water. These measurements indicate that results obtained in dilute conditions as required by many scientific characterization techniques may not be extrapolated to high solids loading slurries for calcium carbonate. Furthermore, these results provide the first explanation for unexplained increases in viscosity of aging slurries at high solids loading.

Keywords: calcium carbonate, slurry, water structure, adsorption, dispersion, sodium polyacrylate, ATR-FTIR, deuterium, oxide, solids, loading, ground

I. Introduction

Ground calcium carbonate (GCC) is used as filler in plastics and papers or as a pigment in paints and coating dispersions. Sodium polyacrylate (NaPAA) is a common polyelectrolyte dispersant used in preparing high solids loading GCC slurries but there is limited knowledge about the interactions between the dispersant, particles, and dispersing medium in high solids loading slurries. GCC and several of its dispersants have been studied under dilute conditions which include measuring zeta potential,[1-10] adsorption isotherms,[1, 3, 8, 11-20] rheological properties,[14, 15, 21-25] and infrared spectroscopy.[20, 26-31] Here, we focus on high solids loading slurries and report unexpected findings of water structure changes.

The objective of this work is to build a scientific foundation for effects that are known in high solid loadings slurries. These slurries are reported by industry experts as being less stable with age, i.e. that a dramatic ageing effect exists that may transform a low viscosity slurry within 4 to 8 weeks into a very high viscosity slurry that limits the emptying of railway cars. This effect is not available in low solids loading slurries. After an extensive literature review it is found that there is no good explanation from dilute systems. However, very high solids loadings are typically not reported in the scientific literature. Therefore, we started to investigate all accessible properties for high solid loading slurries that could possibly lead to colloidal instability. Our surprise finding is reported in this article where we show that calcite slurries have an impact on the structure of water and deuterated water in the slurries. Infrared spectra were recorded in aqueous and deuterated slurries up to 75 ms%. Previous studies of calcite dispersions in dilute conditions did not require consideration of the role of the water structure since changes in water structure do not occur in dilute conditions but become apparent at high solids loading. The change in the properties of the dispersing medium water means that problems that industry faces on a daily basis have not yet been accounted for by the sciences. Other groups have reported on changes in water structure before,[32-36] but have not seen such strong changes as for the here presented calcite slurries. This paper is the first one to address high solids loading calcite slurries.

* Corresponding author: email: wsigm@mse.ufl.edu

II. Experimental

(1) Materials

Ground calcium carbonate (GCC) was provided by Imerys (Sandersville, Georgia) with a d_{50}= 1 µm measured with a sedigraph. The sodium polyacrylate (NaPAA) with molecular weight average M_w=5,967 g/mol (polydispersity 2.04) was provided by Kemira Chemicals, Inc. (Kennesaw, Georgia). Purified water above 16.5 MOhm/cm was used coming from a Barnstead E-pure laboratory water purification system. Deuterium oxide (D_2O), 100.0 atom % D, was purchased from Fisher Scientific (Acros Organics). D_2O is used extensively in this research to reduce infrared (IR) band overlap in critical absorption regions of the dispersant, the dispersing medium and calcite.

(2) Attenuated Total Reflectance – Fourier Transform Infrared (ATR-FTIR)

ATR-FTIR measurements were performed using the Thermo Electron Magna 760 FTIR Microscope with a

ZnSe crystal and a liquid-nitrogen-cooled MCT/A detector. ATR-FTIR spectra were recorded from 650 cm^{-1} to 4000 cm^{-1} with 128 scans and a resolution of 2 cm^{-1}.

(3) Sample Preparation

NaPAA was dissolved in either H_2O or D_2O. Amount of NaPAA in a sample was 1 ms% of the GCC mass. Next, the GCC was slowly added to the solution while stirring with a magnetic stir bar. The mass percent of GCC is a percent of the total GCC plus water mass. The aging samples used for testing were stored in a sealed container during the aging period without agitation.

(4) Spectra Analysis

Deconvolution of the ATR-FTIR spectra was performed by the program PeakFit 4.12. The deconvolution procedure used a Gaussian area nonlinear response function with a Fourier deconvolution algorithm and produced an r^2 value greater than 0.995. Each deconvoluted spectrum's wavenumber, intensity of absorbance, full width at half maximum (FWHM), and sub-area to total area ratio were calculated through PeakFit after successful deconvolution.

III. Results and Discussion

(1) Water Structure and Solids Loading

There are three principal OH and OD vibrational modes of H_2O and D_2O, ν_s, ν_{as}, and δ.[41] The broad transition range between 3100 cm^{-1} - 3600 cm^{-1} for H_2O and 2200 cm^{-1}- 2700 cm^{-1} for D_2O represent the hydroxyl stretching region.[40, 43, 44] As demonstrated in fig. 1, the ATR-FTIR spectrum of a high solids loading GCC slurry is different from the spectrum for bulk water. The strong symmetric absorption around 3200 cm^{-1} generally corresponds to the O-H band with complete tetrahedral coordination (ice-like structure) and the absorption around 3400 cm^{-1} could be assigned to water molecules with incomplete tetrahedral coordination (fluid-like structure).[38, 39] The assignments of hydroxyl group vibrations in the stretching region from literature have been summarized into Table 1. Changes in the spectral features of water are apparent when water is present in a slurry. These changes are demonstrated by comparing the deconvoluted IR bands shown in the first and second row of Table 2. Comparing H_2O to H_2O in a slurry, the water ν_2 band decreases its full width at half maximum (FWHM) and the shoulder at 3178 cm^{-1} shifts to a higher frequency at 3231 cm^{-1}[11] with an 8 % decrease of its intensity of absorbance. Along with the previous changes the ν_3 band is not present in the slurry. Also, the ν_5 band assigned to the free OH vibrations increases the intensity by 16 %. These changes may represent the decreasing strength of hydrogen-bonding and the water structure changes.[40, 50] A difference in the IR spectra of D_2O and D_2O in 75 ms% slurries, fig. 2, resembles the difference seen for H_2O. The IR band of D_2O in slurries decreases its FWHM along with the 2379 cm^{-1} shoulder shifting to 2410 cm^{-1} and the 2492 cm^{-1} shoulder increasing intensity and shifting to 2502 cm^{-1}. Nickolov et al. refer to the lower wavenumber shoulder as ice-like with hydrogen bond coordinations of four and the higher wavenumber shoulder as fluid-like with hydrogen bond coordinations of less than four.[34] The ice-like structure of both H_2O and D_2O in a slurry decreases along with an increase in the fluid-like structure. When water/GCC and water/NaPAA mixtures were measured with ATR-FTIR the spectra do not show any change in the water structure indicating that all three components of the slurry are required for a change in the water structure.

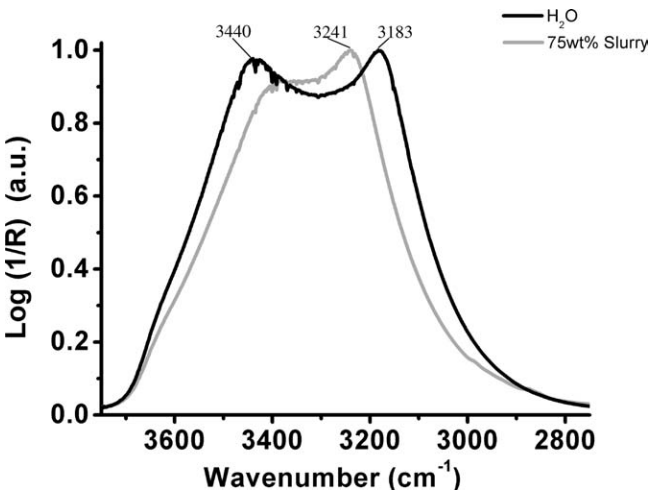

Fig. 1. Attenuated total reflectance-Fourier transform infrared (ATR-FTIR) spectra of the OH stretching band. The change of water structure in a high solids loading slurry (no aging) is shown with a decrease in the full width at half maximum (FWHM) and the shoulder at 3183 cm^{-1} shifting to a higher frequency at 3241 cm^{-1}.

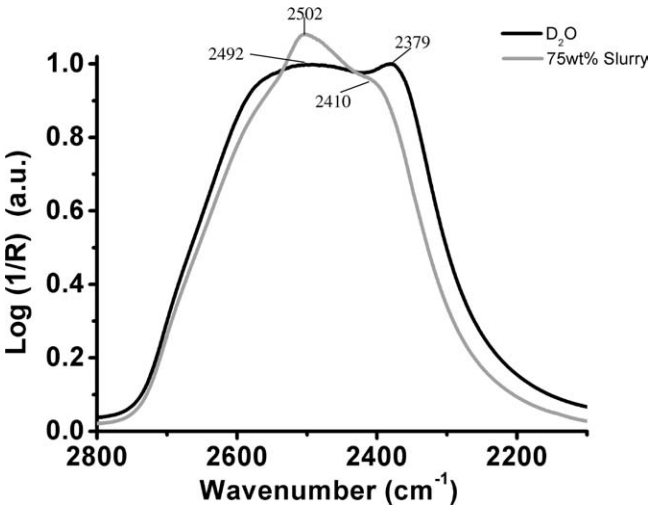

Fig. 2. ATR-FTIR spectra of the OD stretching band. The change of water structure in a high solids loading slurry (no aging) is given by a decrease in the FWHM, the 2379 cm^{-1} shoulder shifting to 2410 cm^{-1}, and the 2492 cm^{-1} shoulder increasing intensity and shifting to 2502 cm^{-1}.

Since it has been concluded that there is a change in the water structure of a 75 ms% slurry compared to bulk water, further investigation was needed to determine if this phenomenon also occurs at lower solids loading. Slurries were prepared containing 10 ms% GCC up to 75 ms% GCC and their IR spectra were compared to a D_2O/GCC mixture without NaPAA. In fig. 3 the intensity of the 10 ms% slurry compared to the D_2O/GCC mixture is

less in the shoulder at 2390 cm^{-1} and greater in the shoulder at 2484 cm^{-1}. Fig. 4 is a graphical representation of the deconvoluted IR spectrum data in Table 2 given for 10 ms% slurry. Since the D_2O/GCC mixture has a higher intensity ν_2 band at 2373 cm^{-1} compared to its ν_4 band at 2551 cm^{-1} we can imply that there is a higher concentration of water in complete tetrahedral networks of hydrogen bonds compared to incomplete networks, which is opposite of a D_2O slurry. Also in fig. 3, increasing the solids loading above 40 ms% increases the 2484 cm^{-1} band intensity (fluid-like structure) and decreases the 2390 cm^{-1} band intensity (solid-like structure). This change is also apparent in Table 2 with the increase of solids loading from 40 ms% up to 75 ms%, the ν_4 band shifts to lower wavenumbers, and increases (5 %) with an accompanying decrease in intensity of the ν_2 band (21 % decrease) and the ν_3 band (decrease to zero). An increase in intensity at higher wavenumbers (fluid-like structure) indicates a decrease in the number of complete tetrahedral hydrogen bonding species (ice-like structure). The reverse trends are displayed by the effect of aging with the concentration of ice-like structures increasing and the concentration of fluid-like structures decreasing with a trend toward bulk water.

Table 1: Major infrared spectrum features of OH and OD vibrations in stretching region.

Solvent	Centered Band (cm^{-1})	Assignment	Ref.
H_2O	~3200	complete tetrahedral coordination (ice-like structure)	34, 36, 48
	3300-3500	inter and intramolecularly uncoupled O-H stretching	45, 46
	~3400	incomplete tetrahedral coordination or less than 4 coordinated	34, 36, 47, 48, 49
	~3600	non-hydrogen-bonding (free OH vibrations)	36, 48, 49
D_2O	~2400	Ice-like structure	36, 42
	~2500	Fluid-like structure	42, 48
	~2650-2750	symmetric and asymmetric of free OD vibrations	42, 48

Table 2: The deconvolution of the OH and OD FTIR spectra into vibrational assignments for several systems.

	Wavenumber/Intensity of Absorbance/FWHM/Area %				
System	ν_1	ν_2	ν_3	ν_4	ν_5
H_2O	3019/0.19/175.3/7.3	3178/0.90/164.5/32.0	3308/0.48/142.9/14.8	3447/0.92/199.6/39.4	3611/0.22/134.8/6.5
H_2O slurry	3091/0.22/183.4/10.8	3231/0.82/156.6/33.2		3387/0.79/179.6/37.6	3540/0.38/187.2/18.4
D2O	2270/0.20/132.1/8.0	2370/0.79/113/26.7	2460/0.61/112.8/20.5	2551/0.79/129/30.5	2646/0.42/115/14.3
D_2O slurry	2297/0.24/110.1/8.9	2389/0.62/105.4/22.3		2502/0.93/151/48.0	2630/0.46/130.6/20.8
D_2O&GCC	2257/0.17/102.3/5.4	2373/0.81/116.4/29.6	2464/0.55/113.3/19.5	2551/0.76/133.7/32.1	2646/0.36/119.6/13.4
10 ms% slurry	2275/0.19/106.6/6.8	2375/0.8/98.9/26.1	2453/0.51/94.3/15.9	2534/0.82/131.4/44.8	2642/0.4/119/15.7
20 ms% slurry	2269/0.17/113.3/6.3	2375/0.8/105.4/27.9	2456/0.42/91.2/12.7	2534/0.84/140/38.6	2648/0.37/118.0/6.8
30 ms% slurry	2272/0.18/118.0/6.8	2379/0.81/113.3/30.1	2459/0.37/89.7/10.7	2534/0.85/135.9/37.8	2646/0.39/116.4/14.7
40 ms% slurry	2287/0.19/130.6/8.0	2384/0.84/116.4/31.0	2470/0.48/89.7/13.4	2549/0.84/132.1/34.8	2653/0.39/107.0/13.1
50 ms% slurry	2285/0.19/123.9/7.9	2381/0.8/105.9/27.9	2457/0.38/80.5/10.0	2528/0.84/131.3/36.5	2637/0.45/119.7/17.7
60 ms% slurry	2274/0.16/114.8/5.9	2380/0.69/122.7/28.5		2509/0.90/160.5/48.5	2634/0.40/125.8/17.0
70 ms% slurry	2285/0.16/116.3/6.6	2384/0.66/116.3/26.9		2503/0.92/144.0/46.3	2628/0.48/120.7/20.2
75 ms% slurry	2258/0.12/99.3/4.3	2380/0.63/126.0/28.2		2506/0.89/157.8/50.3	2637/0.39/122.8/17.3
Aging 1hr	2291/0.16/113.3/6.6	2394/0.60/127.1/28.6		2515/0.89/152.5/49.0	2640/0.39/119.1/16.8
Aging 25hr	2272/0.16/102.3/5.6	2382/0.68/113.3/26.2	2452/0.35/105.4/12.6	2529/0.82/138.4/38.9	2639/0.41/118.9/16.7
Aging 51hr	2276/0.18/116.3/6.8	2383/0.79/113.3/29.1	2467/0.42/108.5/14.6	2543/0.78/141.6/35.5	2646/0.37/116.3/14.0

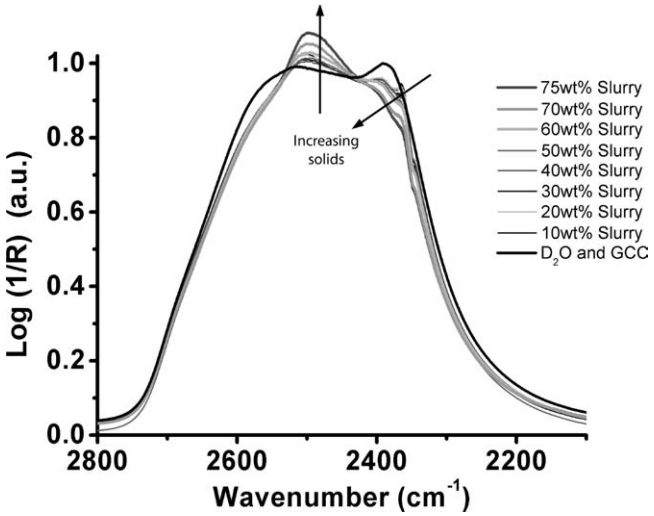

Fig. 3. ATR-FTIR spectra of the OD stretching band. The IR spectra demonstrate that the water structure is dependent on the solids loading of the slurry (no aging). As the solids loading increases there is an increase in the fluid-like structure (~2500 cm^{-1}) and a decrease in the ice-like structure (~2350 cm^{-1}) concentrations.

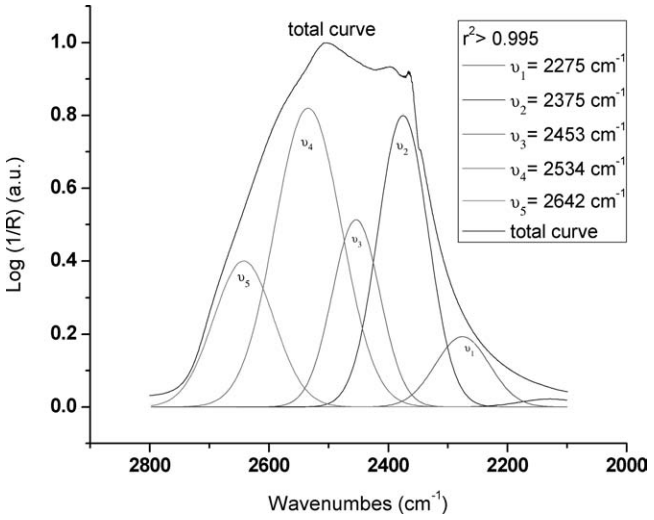

Fig. 4. The deconvolution of the OD stretching infrared absorption spectrum of a 10 ms% slurry in D_2O.

The increase of solids loading might be characterized by the absence of crystalline H-bonding arrangement (ice-like structure) and the shrinkage of the band width might indicate the decrease of the many different H-bonded environments.[41, 42] This change in the ratio of fluid to structured water concentration with increasing solids loading is demonstrated in fig. 5. Two regions are indicated on fig. 5 with the first region ranging from 10 ms% to about 40 ms% (little change in water structure) and the second region which includes concentrations above 40 ms% (indicated with a positive slope which is an increase in the fluid-like water). Fig. 6 is a graphical representation of the deconvoluted FTIR spectra of increasing solids loading from 40 ms% to 60 ms%. The ν_4 band, fluid-like structure, in the shoulder at 2549 cm^{-1} shifts to 2509 cm^{-1} with a 6% intensity increase. Also, with the previous increase there is an observed decrease in the ν_2 band, ice-like structure, intensity of 15% along with the removal of the ν_3 band. The reason for these two regions is not fully understood but could be due to a change in the interaction of the water with the calcium carbonate surface or its adsorbed surface species.

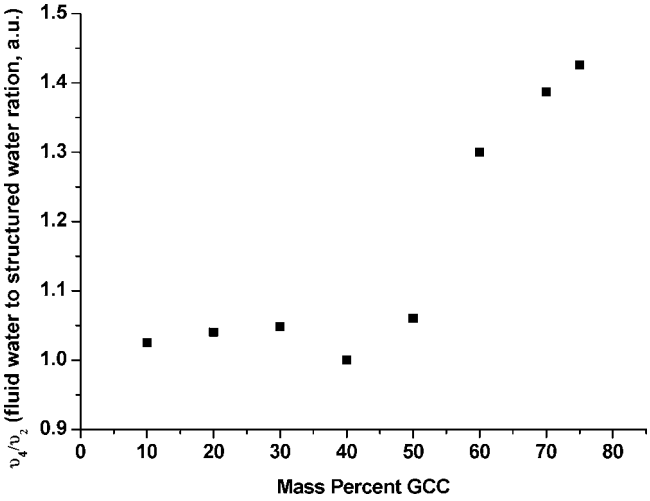

Fig. 5. Solids loading of GCC (no aging) compared to the deconvoluted band ratio ν_4/ν_2 (fluid to structured water ratio). The graph indicates two regions of water structure. The first region includes 10 ms% up to about 40 ms%. The second region includes concentrations above 40 ms% with a positive slope which indicate an increase in the fluid-like water.

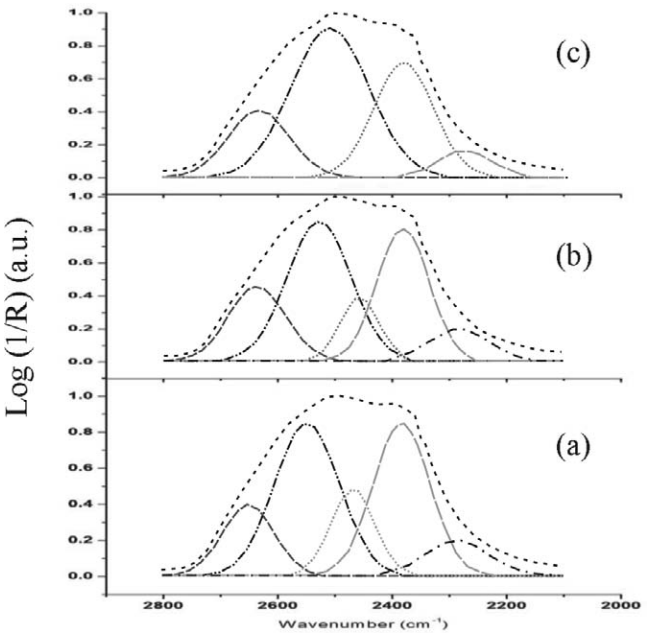

Fig. 6. The deconvolution of the OD stretching infrared absorption spectrum of a (a) 40 ms% (b) 50 ms% (c) 60 ms% slurry. The ν_3 band at ~2470 cm^{-1} in 40 ms% decreases gradually to zero with the increase of solids loading.

(2) Effect of Aging on Water Structure

The properties of the high solids loading slurries change within the first few days of preparing slurries including their viscosity and pH. To determine whether the water structure is a significant part in the aging of high solids loading slurries, samples were prepared and aged followed by measurements and analysis with ATR-FTIR spectroscopy.

Seventy-five ms% slurries were prepared and analyzed on the ATR-FTIR immediately after slurry preparation,

after 25 hrs, and 51 hrs. The results given in fig. 7 indicate that the fluid-like water concentration decreases with increasing age of the high solids loading slurries.

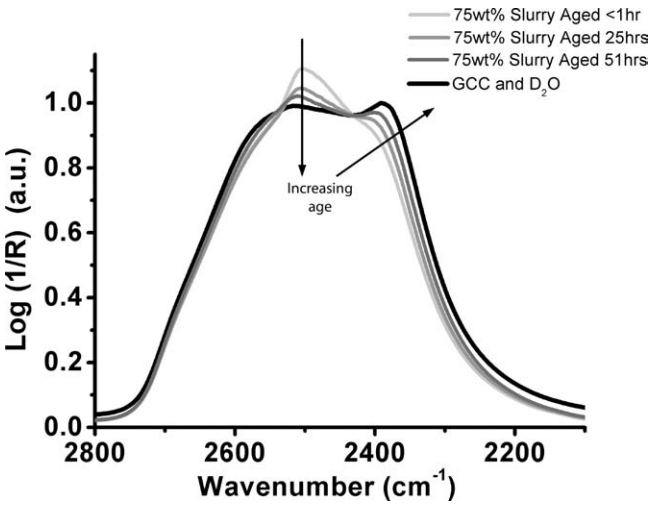

Fig. 7. ATR-FTIR spectra of the OD stretching band. The green line is a freshly prepared 75 ms% GCC slurry. As the age of the slurry increases there is a decrease in the fluid-like structure (~2500 cm^{-1}) and an increase in ice-like structure (~2350 cm^{-1}).

This is seen with a decrease in intensity of the shoulder at 2484 cm^{-1} (fluid-like structure) whereas the shoulder at 2390 cm^{-1} (ice-like structure) increases its intensity. As can be seen in the last three rows of Table 2, the ν_2 band intensity, ice-like structure, increases 19 %, and the ν_4 band, fluid-like structure, decreases 11 %. As the slurry ages it appears to move towards the bulk water structure (black line in fig. 7). The similarities of an aged D_2O to bulk D_2O are also seen in fig. 8 with the deconvoluted OD spectra of a 75 ms% slurry after aging 51 hrs compared to bulk D_2O. It is possible that the O-H vibration of the aged slurry shifts back to the higher frequency indicating a change of the H-bonding strength of the water which is also an indication of the changing slurry physics.[43] It is not clear what guides this process. It appears that water must desorb from certain species to form complete tetrahedral coordination (ice-like structure). This may be possible by rearrangement of ions and polyacrylate dispersants.[37] However, we could not recreate such a condition just using calcium ions and polyacrylate in the proper concentrations. We only see this process taking place in aging slurries with 50 ms% or higher. Furthermore, the aging processes can be reversed quickly. Strongly shearing the slurries almost immediately restores their unaged viscosity as well as returns the ATR-FTIR absorption band intensities close to their fresh slurry status. This indicates that a chemical change is less likely to be the cause of this process.

IV. Conclusions

ATR-FTIR spectroscopy provided evidence that water and deuterium oxide in ground calcium carbonate (GCC) slurries is different from bulk water. The deuterium oxide structure was demonstrated to be dependent on the solids loading of the slurry. Initial addition of all three components; deuterium oxide, sodium polyacrylate (NaPAA), and GCC, increases the intensity ratio of the 2484 cm^{-1} band (fluid-like structure) to the 2390 cm^{-1} band (ice-like structure) compared to bulk deuterium oxide. Increasing solids from 10 ms% up to 40 ms% does not significantly change the water structure but as the solids loading increases above 40 ms% up to 75 ms% the water structure becomes more fluid-like indicated by an increase in the ratio of fluid to ice-like water concentration for higher solids content. Further investigation of GCC slurries were performed at 75 ms% solids loading with aging. Comparison of the IR spectra demonstrates that the water structure becomes more ice-like with increasing age of the slurries. This work concludes that the solids loading directly impacts the dispersing medium for GCC slurries. This finding demonstrates that the interactions in slurries and colloidal systems at high solids loading are different from dilute conditions and may include many other systems.

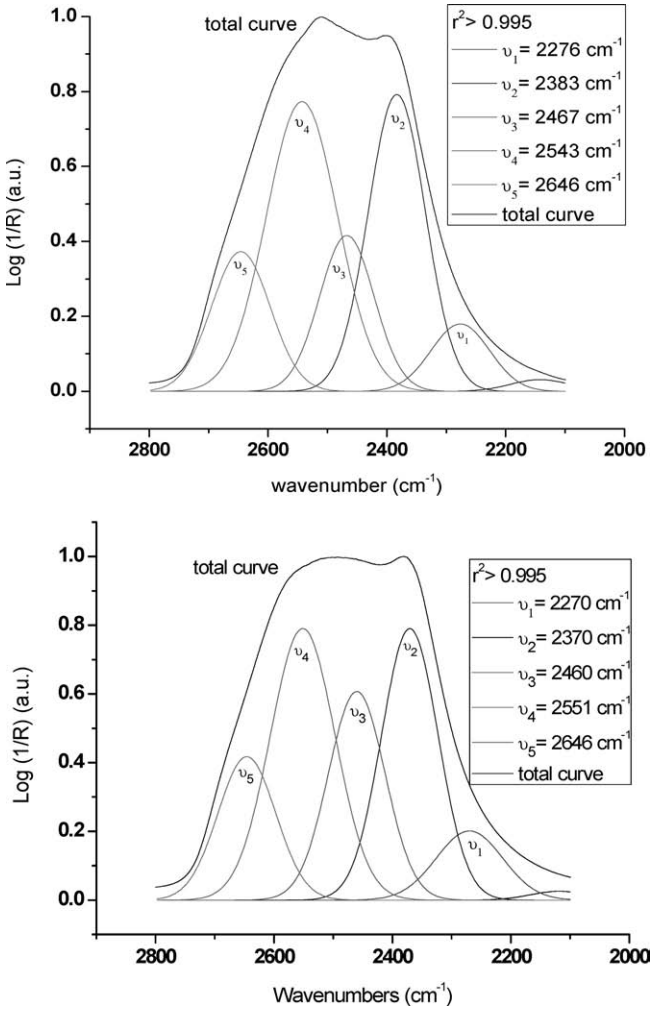

Fig. 8. The deconvolution of the OD stretching infrared absorption spectrum of (a) a 75 ms% slurry in D_2O after aging 51 hrs (b) bulk D_2O. The water structure of an aged slurry is similar to bulk D_2O.

Acknowledgments

This research was supported by an Alumni fellowship of the University of Florida and the dispersion consortium at the Particle Engineering Research Center, including the companies Kemira Chemicals, Inc. and Imerys Clays, Inc.

References

1 Abderrahmen, H. B., Said, H., Partyka, S., Denoyel, R., Ester phosphate adsorption on calcium carbonate, *J. Chim. Phys.-Chim. Biol.*, **94**, 750-764 (1997).

2 Ding, T., Daniels, E. S., El-Aasser, M. S., Klein, A., Surface treatment and characterization of functionalized latex particles and inorganic pigment particles used in the study of film formation from pigmented latex systems, *J. Appl. Polym. Sci.*, **99**, 398-404 (2006).

3 Huang, Y. C., Fowkes, F. M., Lloyd, T. B., Sanders, N. D., Adsorption of Calcium-Ions from Calcium-Chloride Solutions onto Calcium-Carbonate Particles, *Langmuir*, **7**, 1742-1748 (1991).

4 Ivanova, N. I., Shchukin, E. D., Mixed Adsorption of Ionic and Nonionic Surfactants on Calcium-Carbonate, *Colloid Surf. A-Physicochem. Eng. Asp.*, **76**, 109-113 (1993).

5 Knez, S., Klinar, D., Golob, J., Stabilization of PCC dispersions prepared directly in the mother-liquid after synthesis through the carbonation of (hydrated) lime, *Chem. Eng. Sci.*, **61**, 5867-5880 (2006).

6 Moulin, P., Roques, H., Zeta potential measurement of calcium carbonate, *J. Colloid Interface Sci.*, **261**, 115-126 (2003).

7 Saravanan, L., Subramanian, S., Surface chemical studies on the competitive adsorption poly(ethylene glycol) and ammonium poly (methacrylate) onto alumina, *J. Colloid Interface Sci.*, **284**, 363-377 (2005).

8 Song, M. G., Kim, J. Y., Kim, J. D., The dispersion properties of precipitated calcium carbonate suspensions adsorbed with alkyl polyglycoside in aqueous medium, *J. Colloid Interface Sci.*, 226, 83-90 (2000).

9 Song, M. G., Kim, J. Y., Kim, J. D., Effect of sodium stearate and calcium ion on dispersion properties of precipitated calcium carbonate suspensions, *Colloid Surf. A-Physicochem. Eng. Asp.*, **229**, 75-83 (2003).

10 Suty, S., Alince, B., vandeVen, T. G. M., Stability of ground and precipitated CaCO3 suspensions in the presence of polyethylenimine and salt, *J. Pulp Pap. Sci.*, **22**, J321-J326 (1996).

11 Backfolk, K., Lagerge, S., Rosenholm, J. B., Eklund, D., Aspects on the interaction between sodium carboxymethylcellulose and calcium carbonate and the relationship to specific site adsorption, *J. Colloid Interface Sci.*, **248**, 5-12 (2002).

12 Burgess, M. S., Phipps, J. S., Flocculation of PCC induced by polymer/microparticle systems: Floc characteristics, *Nord. Pulp Paper Res. J.*, **15**, 572-578 (2000).

13 Cechova, M., Alince, B., van de Ven, T. G. M., Stability of ground and precipitated CaCO3 suspensions in the presence of polyethylene oxide and kraft lignin, *Colloid Surf. A-Physicochem. Eng. Asp.*, **141**, 153-160 (1998).

14 Chen, J. F., He, T. B., Wu, W., Cao, D. P., Yun, J., Tan, C. K., Adsorption of sodium salt of poly(acrylic) acid (PAANa) on nano-sized CaCO3 and dispersion of nano-sized CaCO3 in water, *Colloid Surf. A-Physicochem. Eng. Asp.*, **232**, 163-168 (2004).

15 El-Sherbiny, S., Xiao, H. N., Effect of polymeric thickeners on pigment coatings: Adsorption, rheological behaviour and surface structures, *J. Mater. Sci.*, **39**, 4487-4493 (2004).

16 Geffroy, C., Persello, J., Foissy, A., Cabane, B., Tournilhac, F., The frontier between adsorption and precipitation of polyacrylic acid on calcium carbonate, *Rev. Inst. Fr. Pet.*, **52**, 183-190 (1997).

17 Nystrom, R., Backfolk, K., Rosenholm, J. B., Nurmi, K., The effect of pretreatment of calcite dispersions with anionic sodium polyacrylate on their flocculation behavior induced by cationic starch, *J. Colloid Interface Sci.*, **262**, 48-54 (2003).

18 Suty, S., Luzakova, V., Role of surface charge in deposition of filler particles onto pulp fibres, *Colloid Surf. A-Physicochem. Eng. Asp.*, **139**, 271-278 (1998).

19 Suzuki, S., Black tea adsorption on calcium carbonate: A new application to chalk powder for brown powder materials, *Colloid Surf. A-Physicochem. Eng. Asp.*, **202**, 81-91 (2002).

20 Vermohlen, K., Lewandowski, H., Narres, H. D., Koglin, E., Adsorption of polyacrylic acid on aluminium oxide: DRIFT spectroscopy and ab initio calculations, *Colloid Surf. A-Physicochem. Eng. Asp.*, 170, 181-189 (2000).

21 Conceicao, S. I., Olhero, S., Velho, J. L., Ferreira, J. M. F., Influence of shear intensity during slip preparation on rheological characteristics of calcium carbonate suspensions, *Ceram. Int.*, 29, 365-370 (2003).

22 Kjeldsen, A. M., Flatt, R. J., Bergstrom, L., Relating the molecular structure of comb-type superplasticizers to the compression rheology of MgO suspensions, *Cem. Concr. Res.*, **36**, 1231-1239 (2006).

23 Kugge, C., Daicic, J., Shear response of concentrated calcium carbonate suspensions, *J. Colloid Interface Sci.*, **271**, 241-248 (2004).

24 Martinelli, G., Plescia, P., Mechanochemical dissociation of calcium carbonate: laboratory data and relation to natural emissions of CO2, *Phys. Earth Planet. Inter.*, **142**, 205-214 (2004).

25 Vorobiev, E., Mouroko-Mitoulou, T., Soua, Z., Precoat filtration of a deflocculated mineral suspension in the presence of a dispersant, *Colloid Surf. A-Physicochem. Eng. Asp.*, **251**, 5-17 (2004).

26 Al-Hosney, H. A., Carlos-Cuellar, S., Baltrusaitis, J., Grassian, V. H., Heterogeneous uptake and reactivity of formic acid on calcium carbonate particles: a Knudsen cell reactor, FTIR and SEM study, *Phys. Chem. Chem. Phys.*, **7**, 3587-3595 (2005).

27 Al-Hosney, H. A., Grassian, V. H., Water, sulfur dioxide and nitric acid adsorption on calcium carbonate: A transmission and ATR-FTIR study, *Phys. Chem. Chem. Phys.*, **7**, 1266-1276 (2005).

28 Bjorklund, R. B., Arwin, H., Jarnstrom, L., Adsorption of Anionic and Cationic Polymers on Porous and Nonporous Calcium-Carbonate Surfaces, *Appl. Surf. Sci.*, **75**, 197-203 (1994).

29 He, P., Bitla, S., Bousfield, D., Tripp, C. P., Raman spectroscopic analysis of paper coatings, *Appl. Spectrosc.*, **56**, 1115-1121 (2002).

30 Kuriyavar, S. I., Vetrivel, R., Hegde, S. G., Ramaswamy, A. V., Chakrabarty, D., Mahapatra, S., Insights into the formation of hydroxyl ions in calcium carbonate: temperature dependent FTIR and molecular modelling studies, *J. Mater. Chem.*, **10**, 1835-1840 (2000).

31 Tabtiang, A., Venables, R., The performance of selected unsaturated coatings for calcium carbonate filler in polypropylene, *Eur. Polym. J.*, **36**, 137-148 (2000).

32 Hancer, M., Celik, M. S., Miller, J. D., The significance of interfacial water structure in soluble salt flotation systems, *J Colloid Interf Sci*, **235**, 150-161 (2001).

33 Nickolov, Z. S., Miller, J. D., Water structure in aqueous solutions of alkali halide salts: FTIR spectroscopy of the OD stretching band, *J Colloid Interf Sci*, **287**, 572-580 (2005).

34 Nickolov, Z. S., Ozcan, O., Miller, J. D., FTIR analysis of water structure and its significance in the flotation of sodium carbonate and sodium bicarbonate salts, *Colloid Surf. A-Physicochem. Eng. Asp.*, **224**, 231-239 (2003).

35 Ozdemir, O., Celik, M. S., Nickolov, Z. S., Miller, J. D., Water structure and its influence on the flotation of carbonate and bicarbonate salts, *J Colloid Interf Sci*, **314**, 545-551 (2007).

36 Ozdemir, O., Karakashev, S. I., Nguyen, A. V., Miller, J. D., Adsorption of carbonate and bicarbonate salts at the air-brine interface, *Int J Miner Process*, **81**, 149-158 (2006).

37 Geffroy, C., Foissy, A., Persello, J., Cabane, B., Surface complexation of calcite by carboxylates in water, *J Colloid Interf Sci*, **211**, 45-53 (1999).

38 Frost, R. L., Kristof, J., Paroz, G. N., Kloprogge, J. T., Role of water in the intercalation of kaolinite with hydrazine, *J Colloidal Interf Sci*, **208**, 216-225 (1998).

39 Du, Q., Freysz, E., Shen, Y. Ron: Surface vibrational spectroscopic studies of hydrogen bonding and hydrophobicity, *Science*, **264**, 826-828 (1994).

40 Deak, J. C., Rhea, S. T., Iwaki, L. K., Dlott, D. D., Vibrational energy relaxation and spectral diffusion in water and deuterated water, *J. Phys. Chem. A*, **104**, 4866-4875 (2000).

41 Clarke, M. J., Harrison, K. L., Johnston, K. P., Howdle, S. M., Water I supercritical carbon dioxide microemulsions: spectro-

scopic investigation of a new environment for aqueous inorganic chemistry, *J. Am. Chem. Soc*., **119**, 6399-6406 (1997).

42 Pandelov, S., Pilles, B. M., Werhahn, J. C., Iglev, H., Time-resolved dynamics of the OH stretching vibration in aqueous NaCl hydrate, *J. Phys. Chem. A*, **113**, 10184-10188 (2009).

43 Noguchi, T., Sugiura, M., Structure of an active water molecule in the water-oxidizing complex of photosystem II as studied by FTIR spectroscopy, *Biochemistry*, **36**, 10943-10949 (2000).

44 Benjamin, Ilan: Vibrational spectrum of water at the liquid/vapor interface, *Phys. Rev. Letters*, **15**, 2083-2086 (1994).

45 Tetsuo Kondo: The assignment of IR absorption bands due to free hydroxyl groups in cellulose, *Cellulose*, **4**, 281-292 (1997).

46 Gragson, D. E., Richmond, G. L., Investigations of the structure and hydrogen bonding of water molecules at liquid surface by vibrational sum frequency spectroscopy, *J. Phys. Chem. B*, **102**, 3447-3861 (1998).

47 Yalamanchili, M. R., Atia, A. A., Miller, J. D., Analysis of interfacial water at a hydrophilic silicon surface by in-situ FTIR/internal reflection spectroscopy, *Langmuir*, **12**, 4176-4184 (1996).

48 Buch, V., Devin, J.P., Spectra of dangling OH bonds in amorphous ice: Assignment to 2- and 3-coordinated surface molecules, *J. Chem. Phys.*, **94**, 4091 (1991).

49 Tsuji, K., Shibuya, K., Infrared spectroscopy and quantum chemical calculations of OH-$(H_2O)_n$ complexs, *J. Phys. Chem. A*, **113**, 9945-9951 (2009).

50 Bailey, J. R., McGuire, M. M., ATR-FTIR observations of water structure in colloidal silica: implications for the hydration force mechanism, *Langmuir*, **23**, 10995-10999 (2007).